Bioorganic & Medicinal Chemistry 19 (2011) 3732–3738

Contents lists available at ScienceDirect

Bioorganic & Medicinal Chemistry

journal homepage: www.elsevier.com/locate/bmc

Conformational variability of different sulfonamide inhibitors with thienyl-acetamido moieties attributes to differential binding in the active site of cytosolic human carbonic anhydrase isoforms ☆

Shyamasri Biswas [a], Mayank Aggarwal [a], Özlen Güzel [b,c], Andrea Scozzafava [c], Robert McKenna [a,*], Claudiu T. Supuran [c,*]

[a] Department of Biochemistry and Molecular Biology, College of Medicine, University of Florida, Box 100245, Gainesville, FL 32610, USA
[b] Istanbul University, Faculty of Pharmacy, Department of Pharmaceutical Chemistry, 34116 Beyazit, Istanbul, Turkey
[c] Università degli Studi di Firenze, Laboratorio di Chimica Bioinorganica, Rm. 188, Via della Lastruccia 3, I-50019 Sesto Fiorentino (Firenze), Italy

ARTICLE INFO

Article history:
Received 28 March 2011
Revised 3 May 2011
Accepted 4 May 2011
Available online 10 May 2011

Keywords:
Carbonic anhydrase
Cytosolic isoforms
Sulfonamide
2-Thienylacetamido tail
X-ray crystallography
Isoform-selective inhibitor

ABSTRACT

The X-ray crystal structures of the adducts of human carbonic anhydrase (hCA, EC 4.2.1.1) II complexed with two aromatic sulfonamides incorporating 2-thienylacetamido moieties are reported here. Although, the two inhibitors only differ by the presence of an additional 3-fluoro substituent on the 4-amino-benzenesulfonamide scaffold, their inhibition profiles against the cytosolic isoforms hCA I, II, III, VII and XIII are quite different. These differences were rationalized based on the obtained X-ray crystal structures, and their comparison with other sulfonamide CA inhibitors with clinical applications, such as acetazolamide, methazolamide and dichlorophenamide. The conformations of the 2-thienylacetamido tails in the hCA II adducts of the two sulfonamides were highly different, although the benzenesulfonamide parts were superimposable. Specific interactions between structurally different inhibitors and amino acid residues present only in some considered isoforms have thus been evidenced. These findings can explain the high affinity of the 2-thienylacetamido benzenesulfonamides for some pharmacologically relevant CAs (i.e., isoforms II and VII) being also useful to design high affinity, more selective sulfonamide inhibitors of various CAs.

1. Introduction

The carbonic anhydrase (CA, EC 4.2.1.1) family of enzymes is widespread in mammals, including humans, and comprises a rather high number of isoforms: primates possess 15 CA isoforms (CA I-CA VA, CA VB–CA XIV) whereas in non primate mammals an additional isoforms, CA XV has been described.[1–6] Many of these enzymes are drug targets.[2] Indeed, CA inhibitors (CAIs) have various clinical applications as diuretic, antiglaucoma, antiobesity or antitumor drugs.[2] CA are responsible for specific physiological functions, and drugs with such a diversity of actions target different CA isozymes.[2–6] Sulfonamides and sulfamates constitute the principal type of classical CAIs,[2] whereas other chemotypes (coumarins, polyamines and phenols), were only recently investigated in detail for such an action.[7–10] The inhibitors of the sulfonamide/sulfamate type bind as anions to the catalytically critical Zn(II) ion from the enzyme active site, also participating in many other interactions (hydrogen bond networks; van der Waals contacts, stacking, etc.) with amino acid residues from the hydrophobic and hydrophilic halves of the enzyme active site, as shown by X-ray crystallographic studies of enzyme–inhibitor complexes.[1–6] X-ray crystal structures are available for many adducts of several isozymes (i.e., CA I, II, IV, VA, VII, IX, XII, XIII and XIV) mostly with sulfonamides, and with several sulfamates/sulfamides.[11] Recently, different families of non-classical inhibitors have also been investigated from the crystallographic viewpoint, allowing for a better understanding of the various inhibition mechanisms of these enzymes.[11]

☆ Coordinates and structure factors have been deposited in the Protein Data Bank as entries 3R16 and 3R17.

* Corresponding authors. Tel.: +1 352 392 5696; fax: +1 352 392 3422 (R.M.); tel.: +39 055 4573005; fax: +39 055 4573385 (C.T.S.).
E-mail addresses: rmckenna@ufl.edu (R. McKenna), claudiu.supuran@unifi.it (C.T. Supuran).

0968-0896/$ - see front matter © 2011 Elsevier Ltd. All rights reserved.
doi:10.1016/j.bmc.2011.05.006

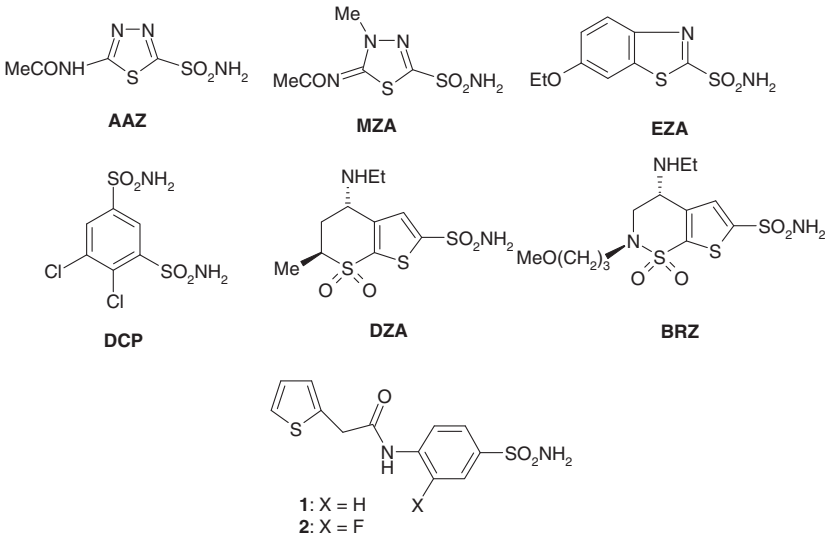

Several sulfonamide CAIs such as acetazolamide **AAZ**, methazolamide **MZA**, ethoxzolamide **EZA** or dichlorophenamide **DCP**, are clinically used as systemic antiglaucoma agents for more than 50 years.[12] More recently, two topically acting antiglaucoma sulfonamides are also available, dorzolamide **DZA** and brinzolamide **BRZ**.[12] However the main drawback of these compounds, and of many sulfonamides reported so far in the literature,[3–6] is their lack of selectivity, as they usually inhibit most of the catalytically active isoforms, in the low nanomolar - micromolar range.[2b,c]

Recently, one of our groups reported a class of aromatic/heterocyclic sulfonamides incorporating 2-thienylacetamido moieties in their molecule, which showed good selectivity ratios for inhibiting some CA isoforms, such as for example CA VII over CA II and I.[13] Among these derivatives, sulfonamides **1** and **2** differing only by the presence of a supplementary fluorine atom in **2** compared to **1**, triggered our attention for several reasons. Both **1** and **2** were observed to be low nanomolar hCA VII (h = human) inhibitors (K_Is in the range of 6.2–7.0 nM), and recently it has been established that this brain-associated cytosolic isoform may be the target of drugs against neuropathic pain.[14] In addition, **1** and **2** were less effective as inhibitors of other two cytosolic isoforms, hCA I and II, which are widespread in many tissues and thus constitute offtargets when the inhibition of other such enzymes are required. Indeed, **1** and **2** showed inhibition constants in the range of 61–161 nM against hCA I and of 50–390 nM against hCA II.[13a] Two issues thus raised regarding the inhibitory properties of these two structurally related compounds: why the presence of a fluorine atom in **2** leads to a hCA II inhibitor 7.8 times less effective compared to **1**? The second question is: why these two compounds show highly effective hCA VII inhibitory activity? In order to address these questions we report here the X-ray crystal structure of the two compounds in complex with hCA II as well as a detailed study for their interactions with all cytosolic CA isoforms, that is, hCA I, II, III, VII and XIII.

2. Results and discussion

2.1. Chemistry and CA inhibition

Sulfonamides **1** and **2** incorporate the thienylacetamido moiety which was shown earlier to be associated with a very potent inhibition of the cytosolic isoforms hCA VII.[13a] Furthermore, these compounds were also shown to act as less effective inhibitors of the widespread cytosolic isoforms hCA I and II,[13a] which constitute offtargets if hCA VII inhibition should be the therapeutic target of interest. Another structural feature of the two compounds is the presence of the sulfanilamide scaffold in their molecule: the unsubstituted sulfanilamide in **1**, and the 3-fluorosulfanilamide in **2**. Thus, the two compounds differ only by the presence of an additional fluorine atom in **2** with respect to **1**, but their inhibition against hCA I and II is rather diverse (Table 1).[13a] Indeed, in the previous work we have assayed the inhibition of compounds **1** and **2** (as well as many other structurally related derivatives) against these three cytosolic isoforms (hCA I, II and VII) of the five presently known. However, two other such cytosolic enzymes are known in humans, the muscle-associated hCA III,[15,16] and the less investigated and understood hCA XIII.[17–20] hCA III was reported to possess a low CO_2 hydrase activity (compared to hCA I and II)[15] and to be also less susceptible to inhibition with sulfonamides, due to the presence of the bulky residues Phe198 in the middle of its active site, which hinders the binding of inhibitors.[15,16] hCA XIII on the other hand has a higher catalytic activity (for the physiologic reaction) compared to hCA III, but at least one order of magnitude lower compared to hCA I and II.[17–19] However, similar to hCA I and II, this isoform is sensitive to sulfonamide inhibitors.[17–19] Indeed, the clinically used drugs such as **AAZ**, **MZA** or **DCP** show inhibition constants in the range of 17–23 nM against CA XIII,[2b] but in the range of 2–7 $\times$ 10^5 nM against CA III.[2b] It appeared thus of interest to investigate how compounds of type **1** and **2** behave against these two less investigated CAs.

Table 1
hCA I, II, III, VII and XIII inhibition data with sulfonamides **1**, **2** and **AAZ**, **MZA** and **DCP** as standard inhibitors, by a stopped-flow CO_2 hydration assay method[20]

Compound	K_I[b] (nM)				
	hCA I[a]	hCA II[a]	hCA III[a]	hCA VII[a]	hCA XIII[a]
1	61	50	8×10^5	6.2	125
2	161	390	12×10^5	7.0	437
AAZ	250	12	2×10^5	2.5	17
MZA	50	14	7×10^5	2.1	19
DCP	1200	38	6.8×10^5	26	23

[a] Recombinant cytosolic isoform.
[b] Errors in the range of ±5–10% of the reported value, from three different determinations.

Data of Table 1 show that compounds **1** and **2** show a weak inhibition of isoform hCA III, similar to all other known sulfonamides [15,16] (K_Is of 8–12 × 10^5 nM) whereas their affinity for hCA XIII is medium, with inhibition constants of 125–437 nM.[20] Thus, compounds **1** and **2** are indeed selective for the inhibition of hCA VII over the other cytosolic isoforms hCA I, II, III and XIII.

2.2. X-ray crystallography

In order to better understand the effect of the placement of a fluorine atom on the benzene ring of 4-substituted-benzenesulfonamide CAIs, X-ray crystallographic studies were performed on **1** and **2** in complex with hCA II. The crystal structures were determined to 1.6 and 1.7 Å resolution, using protocols as previously described.[21,22] Both compounds were refined with full occupancy with B-factors that were comparable to the side chains within the hCA II active site (Table 2). Both compounds displaced the catalytic zinc-bound solvent, such that the sulfonamide amine nitrogen bound directly to the zinc (distance ~2.0 Å). The N and O_2 atoms of the sulfonamide were also within hydrogen bond distances (2.9–3.0 Å) of OG1 and N of Thr199. This observation is consistent with other sulfonamide inhibitors bound to CAs.[2b]

Also both compounds interacted predominantly through Van der Waals contacts with residues Val 121, Phe 131, Val 143, Leu 198, Thr 199, Thr 200, Pro 201, Val 207, Trp 209 and Pro 202, **1** with 349 $Å^2$ (74.5%) and **2** with 359 $Å^2$ (74.0%) of their surface area in contact with hCA II (Fig. 1A, **1** (green) and 1B **2** (cyan)).

For compound **1**, the C5–C4–N7–C8 and C8–N9–C10–C11 torsion angles are −1° and −125°, respectively. The C5–C4–N7–C8 torsion angle is essentially planar and the O8 carbonyl oxygen points towards Gln 92, on the Phe 131 side of the active site. While the C8–N9–C10–C11 torsion angle permits the preceding thiophene ring to be orientated with the sulfur, S14, pointing toward Pro 202, on the opposite side of the active site to Phe 131 (Fig. 1A).

In case of compound **2**, the C5–C4–N7–C8 and C8–N9–C10–C11 torsion angles were 158° and 124°, respectively. The C5–C4–N7–C8 torsion angle, being almost 180° to that of compound **1**. This torsion angle change can be attributed to the fluorine atom, F5, attached to the benzene ring, as having both the F5 and O8 atoms in a *cis*-configuration would create steric hindrance, hence the torsion angle flips to prevent such a clash from occurring. This has the effect of placing the O8 carbonyl oxygen towards Pro 202, away from Phe 131. In addition the C8–N9–C10–C11 torsion angle is rotated, which has the effect of rotating the thiophene ring, to be almost perpendicular to its position observed in compound **1**, although the S14 atom occupies the same spatial location (Fig 1B).

Superposition of the two structures (C_α R.M.S.D. 0.05 Å) reveals that they almost occupy the same volume of the hCA II active site, though the orientation of the O8 carbonyl oxygen points in opposite directions of the active site and the thiophene ring is closer to the Pro 202 and Val 135 for compound **2** (Figs. 1 and 2). Thus, the placement of a fluorine atom on the benzene ring causes a steric clash for compound **2** which is elevated by a *cis* to *trans* transition of the carbonyl oxygen atom and a torsional angle adjustment of the thiophene ring.

2.3. Docking studies of five different inhibitors in hCA VII, hCA III, hCA I and hCA XIII active sites

The X-ray crystal structures of hCA VII[23] and hCA XIII[24a] (in complex with **AAZ**) were recently reported by De Simone's group. Thus, we decided to investigate by docking studies the way in which compounds **1**, **2**, and **AAZ**, **MZA** and **DCP** bind to the cytosolic isoforms hCAI, hCAIII, hCAVII and hCA XIII (Fig. 3).

Compound **2** investigated in the present study was a weaker inhibitor than compound **1** against hCA II, probably because of the presence of the supplementary fluorine atom, which is located in a hydrophobic environment in close proximity to residues Phe131 and Val121 in the hCA II active site. The hydrophobic nature of these residues is conserved across all hCA isoforms investigated here. It is envisageable that the presence of a hydrophilic atom (fluorine) in a hydrophobic enzyme pocket makes **2** a weaker inhibitor in comparison to **1**, which has no halogen atom attached to it. In addition, the carbonyl oxygen O8 of compound **2** points

Table 2
Data reduction and model refinement statistics for the hCA II adducts of sulfonmides **1** and **2**

Data collection statistics		
Compound	**1**	**2**
PDB accession number	3R16	3R17
Temperature (K)	100	100
Wavelength (Å)	1.54	1.54
Spacegroup	$P2_1$	$P2_1$
Unit-cell parameters (Å, °)	a = 42.4, b = 41.4, c = 72, β = 104	a = 42.4, b = 41.3, c = 71.9, β = 104
Total number of measured reflections	114,473	45,252
Total number of unique reflections	30,225	23,896
Resolution (Å)	50–1.6 (1.66–1.6)[d]	50–1.7 (1.76–1.7)[d]
R_{sym}[a]	0.07 (0.27)[d]	0.04 (0.13)[d]
$I/\sigma I$	20.7 (4.9)[d]	16.6 (6.9)[d]
Completeness (%)	93 (87.8)[d]	89 (86.5)[d]
Redundancy	3.8	1.9
Refinement statistics		
R_{work} (%)[b]	15.1	15.1
R_{free} (%)[c]	17.3	19.4
Residue Nos.	257	257
No of protein atoms (including alternate conformations)	2129	2113
No of drug atoms	18	19
No of H_2O molecules	327	283
R.M.S.D: bond lengths (Å), angles (°)	0.006, 1.130	0.006, 1.07
Ramachandran statistics (%): most favored, additionally allowed, and generously allowed regions	97.0, 3.0, 0.0	97.0, 3.0, 0.0
Average B factors ($Å^2$): all, main-, side-chain, ligands, solvent	16.0,12.4, 15.7,19.6, 28.3	19.0,15.8, 19.1,22.2, 29.9

[a] $R_{sym} = \Sigma I - \langle I \rangle / \Sigma \langle I \rangle$.
[b] $R_{work} = (\Sigma |F_o| - |F_c| / \Sigma |F_{obs}|) \times 100$.
[c] R_{free} is calculated in the same manner as R_{work}, except that it uses 5% of the reflection data omitted from refinement.
[d] Values in the parenthesis represents highest resolution bin.

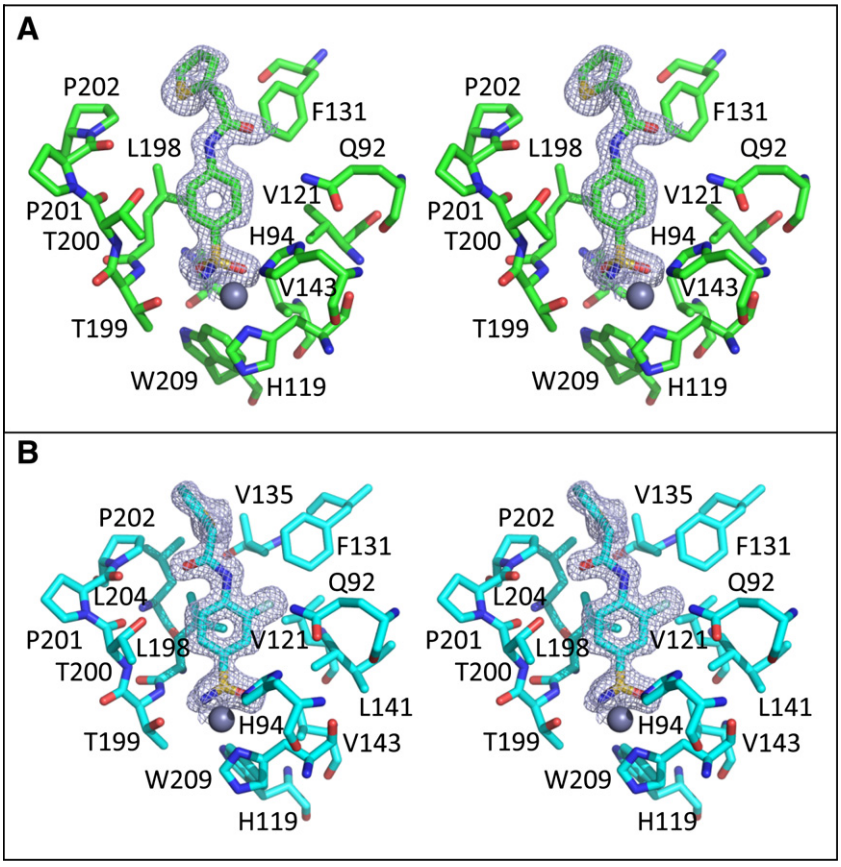

Figure 1. Stereo stick representation of hCA II active site complexed with (A) **1** (green) and (B) **2** (cyan). The active-site zinc is depicted as a gray sphere. The electron density is represented by a 1.2 σ-weighted $2F_o - F_c$ Fourier map (blue mesh). Amino acids are as labeled. Figure made using PyMOL (DeLano Scientific).

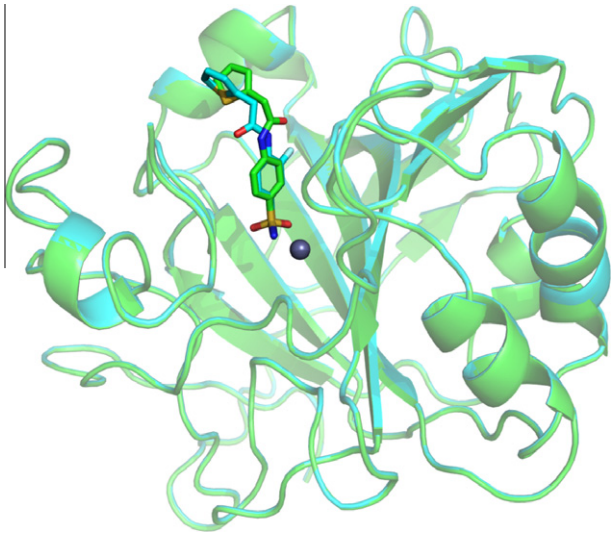

Figure 2. Superposition of hCA II complexed with **1** (green) and **2** (cyan). The zinc is depicted as a gray sphere. Figure made using PyMOL (DeLano Scientific).

towards the carbonyl group of Pro201 of hCA II, thus placing it in a charge repulsive environment, which is not encountered in the hCA II–**1** complex. Here, we have thus a nice example that a relatively minor change in the chemical structure of a sulfonamide CAI has significant consequence to its affinity for the enzyme, strongly influencing its binding within the active site. As we stressed above, the presence of the fluorine makes **2** a 7.8 times less potent hCA II inhibitor compared to the structurally related **1**.

Among all isoforms studied here, the inhibition of hCA III was weaker than that of the other ones (Table 1). The rationale for this is clear, as hCA III has a bulky hydrophobic residue (Phe198) in the middle of the active site cavity, which is a leucine in the other four studied isoforms. This bulky residue effectively prevents any sizable inhibitor to bind into the active site, which is obvious also from Figure 3, showing Phe198 with its bulky phenyl moiety placed in the region where sulfonamides bind in the adducts with other cytosolic isoforms, such as hCA I, II and XIII.

The present data also showed that the best inhibition with compounds **1** and **2** was against hCA VII (Table 1). This potent inhibition is probably due to the presence of Lys93 in hCA VII, an amino acid residue which is unique only to this isoform, providing a hydrophilic and flexible amino acid residue in the middle of the active site, which furnish an additional interaction point for the inhibitor. Based on a model generated using *Coot*,[29] Lys93 can have an alternate conformation leading to the formation of a hydrogen bond with either the carbonyl oxygen of compound **1** or the fluorine atom present in compound **2**, thereby further stabilizing the inhibitor–hCA VII complexes. When this residue is replaced by a bulky side chain such as Arg91 (in the case of hCA XIII and hCA III) the inhibition with compounds **1** and **2** is weaker compared to hCA VII, most likely because the flexibility of Arg91 is reduced compared to that of the lysine present in hCA VII, also leading to steric clashes. In addition, hCA VII also has a smaller side chain (Ala137) close to the active site instead of hydrophobic, bulkier Val135 (present in hCA II and XIII), which might facilitate the easier binding of inhibitors within the hCA VII active site. The observation that Lys93 could be involved in a possible additional hydrogen bond for the hCA VII adducts of these inhibitors might be extended also to the other

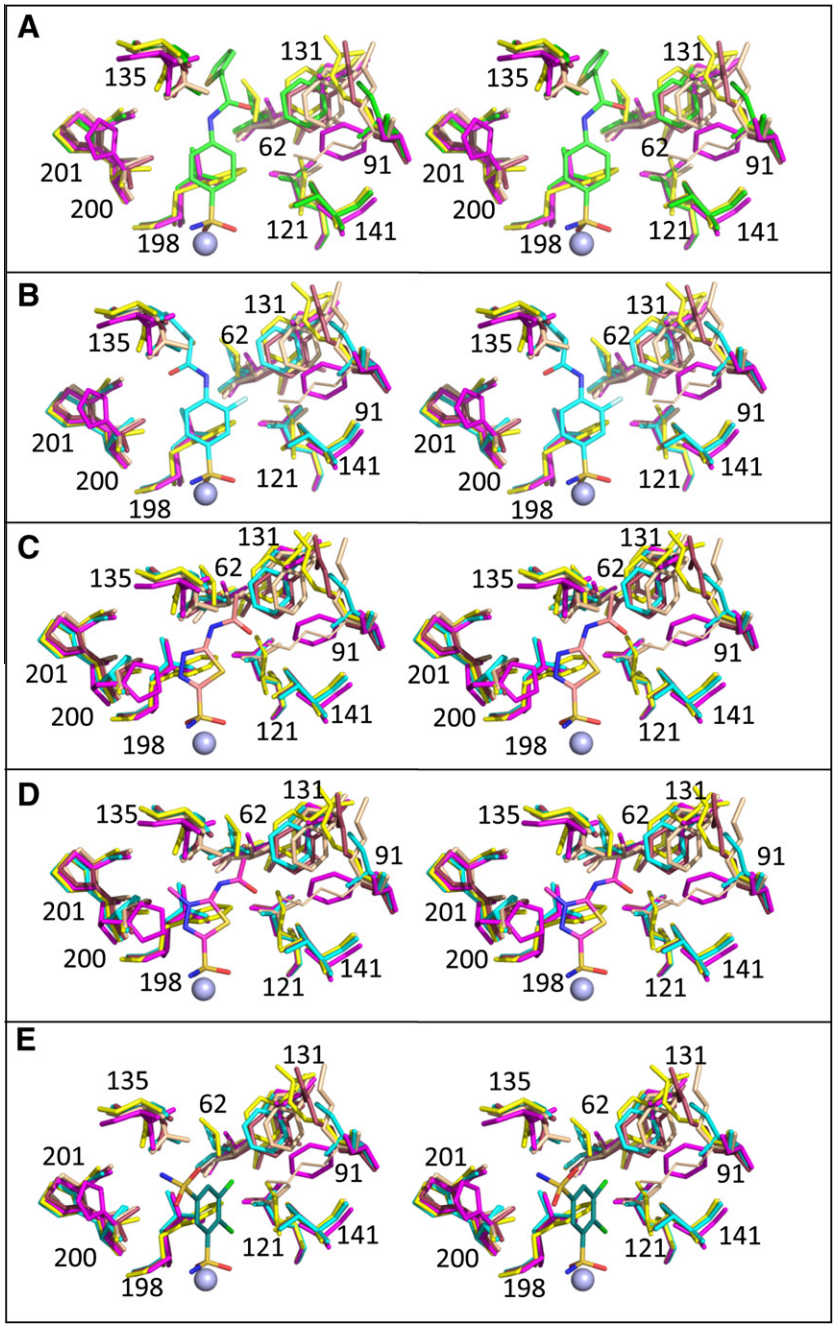

Figure 3. Stereo stick representation of the superposition of hCA I (pink), hCA II (green), hCA III (yellow), hCA VII (wheat), and hCA XIII (purple) active sites complexed with (A) **1**, (B) **2**, (C) **AAZ**, (D) **MZA**, and (E) **DCP**. The active-site zinc is depicted as a gray sphere. Amino acids positions are labeled using hCA II numbering. Figure made using PyMOL (DeLano Scientific).

compounds studied, such as **AAZ**, **MZA**, **DCP**. This fact was corroborated by the lower K_Is measured for these sulfonamides against this isoform (compared to hCA I, II, III and XIII), which is the most inhibited by sulfonamides among all the cytosolic CAs (Table 1).

Excluding the poor inhibition of hCA III observed for all studied compounds, **DCP** showed the weakest inhibition against hCA I among the other cytosolic isoforms (Table 1). This is the only inhibitor used in the present studies bearing two sulfonamide moieties, and its X-ray structure in complex with hCA II was reported earlier by one of our groups.[24b] In the case of hCA I, the residues closest to the second sulfonamide moiety of **DCP** were His200 and Val62 (Fig. 3), which correspond to Thr202 and Asn62 in case of hCA II. The presence of the sulfonamide group close to His200 may result in charge repulsions, leading to the observed weaker inhibition of **DCP** against hCA I (Table 1). On the other hand, the presence of Asn62 in case of hCA II (which is highly polar and flexible), can stabilize interactions with a sulfonamide group close to it, thus making **DCP** a rather potent inhibitor for hCA II, hCA VII and hCA XIII (compared to hCA I and III). The presence of the bulky side chain residue His200 in the hCA I active site also leads to a 20 fold decrease in inhibition with **AAZ** compared to hCA II. However in case of the **MZA**–hCA I complex, the presence of the additional methyl group of the inhibitor in the hydrophobic pocket makes it a better inhibitor of hCA I compared **AAZ**. Collectively these results help us understand the affinity/selectivity of different sulfonamide inhibitors towards the cytosolic CA isoforms, which show a great

variation in their inhibition profile for this class of pharmacologically important compounds, even in the presence of minimal structural changes of inhibitors, such as; the comparison of **1** having a better K_I than **2** for all the CA isoforms tested, and **MZA** exhibiting selectivity over **AAZ** only for hCA I (Fig. 3).

3. Conclusions

The X-ray crystal structure of the adducts of hCA II complexed with two aromatic sulfonamides incorporating 2-thienylacetamido moieties is reported here. The two inhibitors only differ by the presence of an additional 3-fluoro substituent on the 4-amino-benzenesulfonamide scaffold of one of them, but their inhibition profiles against the cytosolic isoforms hCA I, II, III, VII and XIII are quite different. These differences were rationalized based on the obtained X-ray crystal structures, including in the comparison other sulfonamide CA inhibitors with clinical applications, such as **AAZ**, **MZA** and **DCP**. Specific interactions between the structurally different inhibitors and amino acid residues present only in some of these isoforms have been shown, which explain the high affinity of the 2-thienylacetamido benzenesulfonamides for some pharmacologically relevant CAs such as isoforms II and VII, and might be useful for the drug design of isoform-selective sulfonamide inhibitors of various CAs.

4. Experimental

4.1. Chemistry and CA inhibition

Sulfonamides used in this work were reported earlier (**1** and **2**)[13] or are commercially available from Sigma-Aldrich (Milan, Italy). An Applied Photophysics stopped-flow instrument has been used for assaying the CA catalysed CO_2 hydration activity. Phenol red (at a concentration of 0.2 mM) has been used as indicator, working at the absorbance maximum of 557 nm, with 20 mM Hepes (pH 7.5) as buffer, and 20 mM Na_2SO_4 (for maintaining constant the ionic strength), following the initial rates of the CA-catalyzed CO_2 hydration reaction for a period of 10–100 s. The CO_2 concentrations ranged from 1.7 to 17 mM for the determination of the kinetic parameters and inhibition constants. For each inhibitor at least six traces of the initial 5–10% of the reaction have been used for determining the initial velocity. The uncatalyzed rates were determined in the same manner and subtracted from the total observed rates. Stock solutions of inhibitor (0.1 mM) were prepared in distilled-deionized water and dilutions up to 0.01 nM were done thereafter with distilled-deionized water. Inhibitor and enzyme solutions were preincubated together for 15 min at room temperature prior to assay, in order to allow for the formation of the E–I complex. The inhibition constants were obtained by non-linear least-squares methods using PRISM 3, as reported earlier,[13] and represent the mean from at least three different determinations. CA isoforms were recombinant ones obtained in house as reported earlier.[7–10,13]

4.2. X-ray crystal structure determination

hCA II was purified to electrophoretic homogeneity according to previously described protocol.[3] Co-crystals of the hCA II – **1**, – **2** complexes were obtained using the hanging drop vapor diffusion method.[25] Drops of 5 μL (0.5 mM hCA II; 1 mM compound; 0.1% dimethyl sulfoxide (DMSO); 0.8 M Sodium Citrate; 50 mM Tris–HCl; pH 8.0) were equilibrated against 1 ml precipitant solution (1.6 M sodium citrate; 50 mM Tris–HCl; pH 8.0) at room temperature (~20 °C). Prior to collecting X-ray diffraction datasets, the crystal were cryoprotected using 25% glycerol in the precipitant solution containing 2 mM drug solution and flash cooled in gaseous nitrogen stream. Data were collected at 100 K using a R-AXIS IV^{++} image plate (IP) system with OsmicVarimax optics and a Rigaku RU-H3R Cu rotating anode operating at 50 kV and 22 mA. The crystal to IP distance was 76 mm in case of compound **1** and 80 mm in case of compound **2**. The oscillation steps were 1° with 5 min exposure per image. Indexing, integration and scaling were performed using HKL2000.[26]

The structures of hCAII bound to compound **1** and **2** were solved by using hCAII as a model (PDB accession code 2ILI).[2d] Initial phases were obtained by molecular substitution using PHASER in ccp4 suite.[27] Refinement proceeded with 5% of the data allocated for R_{free} calculations using PHENIX version 1.7.[28] The ligand coordinates were generated using eLBOW in PHENIX and subsequently merged using Coot.[29] After several cycles of refinement alternated with manual refitting of the model and solvent placement the models converged. The validity of the final model was assessed by *PROCHECK*.[30] Complete refinement statistics are included in Table 2.

4.3. Structure–activity relationship and alignment of different CA isoforms

The hCA I (PDB accession number 3LXE),[31] VII (PDB accession number 3ML5)[23] and XIII (PDB accession number 3CZV)[24a] coordinates were superimposed onto hCA II complexed with compounds **1**, **2**, **AAZ**, **MZA** and **DCP**. The align option in PyMOL was used to superimpose different CA isoform structures. This feature in PyMOL calculates the RMSD values for different superimposed structures and makes a best possible alignment of them. In case of compounds **1** and **2** the hCAII structure reported here was used as a reference structure and various CA isoform structures without ligands were superimposed onto them. Similarly the hCAII structure in complex with **DCP** (2POU) was used as a reference structure to generate Figure 3E. In case of **AAZ** and **MZA**, hCA VII structure (3ML5) and hCAI (1BZM), respectively, were used as the reference, all other unliganded forms of CA were used as the moving structures for superposition. After aligning the structures in PyMOL the active site residues were highlighted and shown in stick form (Fig. 3). The differences in amino acids at various inhibitor-interaction regions was also analyzed using the SSM superpose option in *Coot*.[29] The figures were made using PyMOL.[32]

References and notes

1. Hilvo, M.; Tolvanen, M.; Clark, A.; Shen, B.; Shah, G. N.; Waheed, A.; Halmi, P.; Hänninen, M.; Hämäläinen, J. M.; Vihinen, M.; Sly, W. S.; Parkkila, S. *Biochem. J.* **2005**, *392*, 83.
2. (a) Kaunisto, K.; Parkkila, S.; Rajaniemi, H.; Waheed, A.; Grubb, J.; Sly, W. S. *Kidney Int.* **2002**, *61*, 2111; (b) Supuran, C. T. *Nat. Rev. Drug Disc.* **2008**, *7*, 168; (c) Supuran, C. T. *Bioorg. Med. Chem. Lett.* **2010**, *20*, 3467; (d) Fisher, S. Z.; Maupin, C. M.; Budayova-Spano, M.; Govindasamy, L.; Tu, C. K.; Agbandje-McKenna, M.; Silverman, D. N.; Voth, G. A.; McKenna, R. *Biochemistry* **2007**, *42*, 2930; (e) Ebbesen, P.; Pettersen, E. O.; Gorr, T. A.; Jobst, G.; Williams, K.; Kienninger, J.; Wenger, R. H.; Pastorekova, S.; Dubois, L.; Lambin, P.; Wouters, B. G.; Supuran, C. T.; Poellinger, L.; Ratcliffe, P.; Kanopka, A.; Görlach, A.; Gasmann, M.; Harris, A. L.; Maxwell, P.; Scozzafava, A. *J. Enzyme Inhib. Med. Chem.* **2009**, *24*, 1.
3. (a) Wagner, J. M.; Avvaru, B. S.; Robbins, A. H.; Scozzafava, A.; Supuran, C. T.; McKenna, R. *Bioorg. Med. Chem.* **2010**, *18*, 4873; (b) Pacchiano, F.; Aggarwal, M.; Avvaru, B. S.; Robbins, A. H.; Scozzafava, A.; McKenna, R.; Supuran, C. T. *Chem. Commun. (Camb.)* **2010**, *46*, 8371; (c) Pastorekova, S.; Parkkila, S.; Pastorek, J.; Supuran, C. T. *J. Enzyme Inhib. Med. Chem.* **2004**, *19*, 199; (d) Poulsen, S. A. *Expert Opin. Ther. Pat.* **2010**, *20*, 795; (e) Alterio, V.; Hilvo, M.; Di Fiore, A.; Supuran, C. T.; Pan, P.; Parkkila, S.; Scaloni, A.; Pastorek, J.; Pastorekova, S.; Pedone, C.; Scozzafava, A.; Monti, S. M.; De Simone, G. *Proc. Natl. Acad. Sci. U.S.A.* **2009**, *106*, 16233.
4. (a) Supuran, C. T. Carbonic Anhydrases as Drug Targets—General Presentation. In *Drug Design of Zinc-Enzyme Inhibitors: Functional, Structural, and Disease Applications*; Supuran, C. T., Winum, J. Y., Eds.; Wiley: Hoboken (NJ), 2009; pp 15–38; (b) Winum, J. Y.; Rami, M.; Scozzafava, A.; Montero, J. L.; Supuran, C. *Med. Res. Rev.* **2008**, *28*, 445; (c) Supuran, C. T.; Scozzafava, A.; Casini, A. *Med. Res. Rev.* **2003**, *23*, 146.

5. (a) De Simone, G.; Di Fiore, A.; Menchise, V.; Pedone, C.; Antel, J.; Casini, A.; Scozzafava, A.; Wurl, M.; Supuran, C. T. *Bioorg. Med. Chem. Lett.* **2005**, *15*, 2315; (b) Casini, A.; Antel, J.; Abbate, F.; Scozzafava, A.; David, S.; Waldeck, H.; Schafer, S.; Supuran, C. T. *Bioorg. Med. Chem. Lett.* **2003**, *13*, 841; (c) Abbate, F.; Casini, A.; Owa, T.; Scozzafava, A.; Supuran, C. T. *Bioorg. Med. Chem. Lett.* **2004**, *14*, 217; (d) Abbate, F.; Casini, A.; Scozzafava, A.; Supuran, C. T. *Bioorg. Med. Chem. Lett.* **2004**, *14*, 2357.
6. (a) Winum, J. Y.; Casini, A.; Mincione, F.; Starnotti, M.; Montero, J. L.; Scozzafava, A.; Supuran, C. T. *Bioorg. Med. Chem. Lett.* **2004**, *14*, 225; (b) Menabuoni, L.; Scozzafava, A.; Mincione, F.; Briganti, F.; Mincione, G.; Supuran, C. T. *J. Enzyme Inhib.* **1999**, *14*, 457; (c) Scozzafava, A.; Menabuoni, L.; Mincione, F.; Briganti, F.; Mincione, G.; Supuran, C. T. *J. Med. Chem.* **1999**, *42*, 2641.
7. Carta, F.; Temperini, C.; Innocenti, A.; Scozzafava, A.; Kaila, K.; Supuran, C. T. *J. Med. Chem.* **2010**, *53*, 5511.
8. (a) Maresca, A.; Temperini, C.; Vu, H.; Pham, N. B.; Poulsen, S. A.; Scozzafava, A.; Quinn, R. J.; Supuran, C. T. *J. Am. Chem. Soc.* **2009**, *131*, 3057; (b) Maresca, A.; Temperini, C.; Pochet, L.; Masereel, B.; Scozzafava, A.; Supuran, C. T. *J. Med. Chem.* **2010**, *53*, 335.
9. (a) Maresca, A.; Supuran, C. T. *Bioorg. Med. Chem. Lett.* **2010**, *20*, 4511; (b) Maresca, A.; Scozzafava, A.; Supuran, C. T. *Bioorg. Med. Chem. Lett.* **2010**, *20*, 7255.
10. Innocenti, A.; Vullo, D.; Scozzafava, A.; Supuran, C. T. *Bioorg. Med. Chem. Lett.* **2008**, *18*, 1583.
11. Alterio, V.; Di Fiore, A.; D'Ambrosio, K.; Supuran, C. T.; De Simone, G. X-Ray Crystallography of CA Inhibitors and Its Importance in Drug Design. In *Drug Design of Zinc-Enzyme Inhibitors: Functional, Structural, and Disease Applications*; Supuran, C. T., Winum, J. Y., Eds.; Wiley: Hoboken, 2009; pp 73–138.
12. (a) Wistrand, P. J.; Lindqvist, A. In *Carbonic Anhydrase—From Biochemistry and Genetics to Physiology and Clinical Medicine*; Botrè, F., Gros, G., Storey, B. T., Eds.; VCH: Weinhein, 1991; pp 352–378; (b) Mincione, F.; Scozzafava, A.; Supuran, C. T. Antiglaucoma Carbonic Anhydrase Inhibitors as Ophthalomologic Drugs. In *Drug Design of Zinc-Enzyme Inhibitors: Functional, Structural, and Disease Applications*; Supuran, C. T., Winum, J. Y., Eds.; Wiley: Hoboken (NJ), 2009; pp 139–154; (c) Steele, R. M.; Batugo, M. R.; Benedini, F.; Biondi, S.; Borghi, V.; Carzaniga, L.; Impagnatiello, F.; Miglietta, D.; Chong, W. K. M.; Rajapakse, R.; Cecchi, A.; Temperini, C.; Supuran, C. T. *Bioorg. Med. Chem. Lett.* **2009**, *19*, 6565.
13. (a) Güzel, Ö.; Innocenti, A.; Scozzafava, A.; Salman, A.; Supuran, C. T. *Bioorg. Med. Chem. Lett.* **2009**, *19*, 3170; (b) Güzel, Ö.; Innocenti, A.; Scozzafava, A.; Salman, A.; Supuran, C. T. *Bioorg. Med. Chem.* **2009**, *17*, 4894.
14. Asiedu, M.; Ossipov, M. H.; Kaila, K.; Price, T. J. *Pain* **2010**, *148*, 302.
15. (a) Wistrand, P. J. *Ups. J. Med. Sci.* **2002**, *107*, 77; (b) Carter, N.; Shiels, A.; Tashian, R. *Biochem. Soc. Trans.* **1978**, *6*, 552; (c) Elder, I.; Fisher, Z.; Laipis, P. J.; Tu, C.; McKenna, R.; Silverman, D. N. *Proteins* **2007**, *68*, 337; (d) Duda, D. M.; Tu, C.; Fisher, S. Z.; An, H.; Yoshioka, C.; Govindasamy, L.; Laipis, P. J.; Agbandje-McKenna, M.; Silverman, D. N.; McKenna, R. *Biochemistry* **2005**, *44*, 10046.
16. (a) Nishimori, I.; Minakuchi, T.; Onishi, S.; Vullo, D.; Cecchi, A.; Scozzafava, A.; Supuran, C. T. *Bioorg. Med. Chem.* **2007**, *15*, 7229; (b) Nishimori, I.; Minakuchi, T.; Onishi, S.; Vullo, D.; Cecchi, A.; Scozzafava, A.; Supuran, C. T. *J. Enzyme Inhib. Med. Chem.* **2009**, *24*, 70.
17. (a) Lehtonen, J.; Shen, B.; Vihinen, M.; Casini, A.; Scozzafava, A.; Supuran, C. T.; Parkkila, A.-K.; Saarnio, J.; Kivelä, A.; Waheed, A.; Sly, W. S.; Parkkila, S. *J. Biol. Chem.* **2004**, *279*, 2719; (b) Lehtonen, J. M.; Parkkila, S.; Vullo, D.; Casini, A.; Scozzafava, A.; Supuran, C. T. *Bioorg. Med. Chem. Lett.* **2004**, *14*, 3757.
18. Hilvo, M.; Supuran, C. T.; Parkkila, S. *Curr. Top. Med. Chem.* **2007**, *7*, 893.
19. Hilvo, M.; Innocenti, A.; Monti, S. M.; De Simone, G.; Supuran, C. T.; Parkkila, S. *Curr. Pharm. Des.* **2008**, *14*, 672.
20. Khalifah, R. G. *J. Biol. Chem.* **1971**, *246*, 2561.
21. Avvaru, B. S.; Wagner, J. M.; Maresca, A.; Scozzafava, A.; Robbins, A. H.; Supuran, C. T.; McKenna, R. *Bioorg. Med. Chem. Lett.* **2010**, *20*, 4376.
22. (a) Di Fiore, A.; De Simone, G.; Menchise, V.; Pedone, C.; Casini, A.; Scozzafava, A.; Supuran, C. T. *Bioorg. Med. Chem. Lett.* **2005**, *15*, 1937; (b) Menchise, V.; De Simone, G.; Alterio, V.; Di Fiore, A.; Pedone, C.; Scozzafava, A.; Supuran, C. T. *J. Med. Chem.* **2005**, *48*, 5721; (c) Baranauskiene, L.; Hilvo, M.; Matuliene, J.; Golovenko, D.; Manakova, E.; Dudutiene, V.; Michailoviene, V.; Torresan, J.; Jachno, J.; Parkkila, S.; Maresca, A.; Supuran, C. T.; Grazulis, S.; Matulis, D. *J. Enzyme Inhib. Med. Chem.* **2010**, *25*, 863; (d) Di Fiore, A.; Monti, S. M.; Innocenti, A.; Winum, J.-Y.; De Simone, G.; Supuran, C. T. *Bioorg. Med. Chem. Lett.* **2010**, *20*, 3601.
23. Di Fiore, A.; Truppo, E.; Supuran, C. T.; Alterio, V.; Dathan, N.; Bootorabi, F.; Parkkila, S.; Monti, S. M.; De Simone, G. *Bioorg. Med. Chem. Lett.* **2010**, *20*, 5023.
24. (a) Di Fiore, A.; Monti, S. M.; Hilvo, M.; Parkkila, S.; Romano, V.; Scaloni, A.; Pedone, C.; Scozzafava, A.; Supuran, C. T.; De Simone, G. *Proteins* **2009**, *74*, 164; (b) Alterio, V.; De Simone, G.; Monti, S. M.; Scozzafava, A.; Supuran, C. T. *Bioorg. Med. Chem. Lett.* **2007**, *17*, 4201.
25. McPherson, A. *Preparation and Analysis of Protein Crystals*, 1st ed.; Wiley: New York, 1982.
26. Otwinowski, Z.; Minor, W. *Methods Enzymol.* **1997**, *276*, 307.
27. Collaborative Computational Project, Number 4. *Acta Crystallogr., Sect. D*, **1994**, *50*, 760.
28. Adams, P. D.; Afonine, P. V.; Bunkóczi, G.; Chen, V. B.; Davis, I. W.; Echols, N.; Headd, J. J.; Hung, L.-W.; Kapral, G. J.; Grosse-Kunstleve, R. W.; McCoy, A. J.; Moriarty, N. W.; Oeffner, R.; Read, R. J.; Richardson, D. C.; Richardson, J. S.; Terwilliger, T. C.; Zwart, P. H. *Acta Crystallogr., Sect. D* **2010**, *66*, 213.
29. Emsley, P.; Cowtan, K. *Acta Crystallogr., Sect. D* **2004**, *60*, 2126.
30. Laskowski, R. A.; MacArthur, M. W.; Moss, D. S.; Thornton, J. M. *J. Appl. Crystallogr.* **1993**, *26*, 283.
31. Alterio, V.; Monti, S. M.; Truppo, E.; Pedone, C.; Supuran, C. T.; De Simone, G. *Org. Biomol. Chem.* **2010**, *8*, 3528.
32. The PyMOL Molecular Graphics System, Version 1.3, Schrödinger, LLC.